One Dimensional Elastic Infinite Composite Media Discretized by Boundary Point Method Explored from the Convergence Point of View

Jan Novák

***Abstract*—Nowadays a number of computational methods to estimate the mechanical fields inside the composite materials are available. Usually the main role plays the Finite Element Method and the periodic field assumption. On the other hand, there exists a number of applications in engineering practice where a strongly non-periodic character of composite medium can be also encountered (e.g. biological materials, foams, concrete, etc.). Then it becomes to be convenient to use the infinite medium with separated inclusions theory. Similarly to previous works of Maz'ya, Kanaoun, Romero etc. the theory of integral equations and their discretization using Gauss approximating functions is presented. The influence of the nodal discretization refinement or the initial setup of an H–dimensionless parameter on the quality of final approximation is also discussed.**

The method itself produces due to a regular discretization grid the Toeplitz structured matrices. Such systems can be advantageously solved using iterative solvers based on Fast Fourier Transform technique. On the other hand, although less efficient, direct solvers exhibit other advantages and can be used with great benefit in the case of ill-posed systems.

The effort of this work is to point out the main benefits and difficulties of the Boundary Point Method application on the simplest one-dimensional example.

***Index Terms*—Boundary Point Method, Boundary Element Method, perturbation, infinite media, inclusion, integral equation, composite media, heterogeneous materials**

I. Introduction

THE Boundary Point Method (BPM) is a quite new numerical approach designed for a solution of various problems of applied mathematics and physics. It was introduced by Russian mathematician Maz'ya [1, 2] in the nineties of the last century. Contrary to a very popular Finite Element Method (FEM) discretizing differential equations, the BPM is based on the discretization of integral equations. From the heterogeneous materials behavior point of view the BPM is on continuous rise predominantly in the academic sphere, see e.g. Kanaun et al. [3, 4, 5].

This article shows various aspects of BPM on the simplest one-dimensional case, here the work [6] is refered to see the benefits of such an approach. In particular, the presented problem starts from the formulation of basic equilibrium equation of a 1D isotropic elastic deformable body. Consequently, the infinite 1D composite medium is introduced and followed by the boundary point discretization of the strain field. One of the main topics of this contribution lies in the convergence study of the resulting global system of linear equations.

The paper is structured as follows. First, the formulation of basic constitutive equations of both homogeneous and heterogeneous elastic body is briefly reviewed in section **II**. The next section **III** deals with the problem solution defined et the end of section **II** that is particularly the solution of unknown strain inside the heterogeneous body occupied by one and more inclusions. Then, section **IV** describes the BPM approximation concept using Gauss approximate functions and shows the linearization procedure on well known $\sin(x)$ function. Discretization of unknown strain field at final number of boundary nodes follows. Comparisons of the exact solution with the numerical one from a number of viewpoints is then presented in section **V**. Among other things, this section also contains the confrontation of direct and iterative solver, respectively. Finally, various conclusions of numerical experiments with some proposals to future work are given in sec. **VI**.

II. Basic equations of elastic body

A. Homogeneous elastic body

With reference to Fig. 1 an infinite rod of a unit crossectional area A is considered. Such a rod is loaded by constant strain ε^0 at ∞ and $-\infty$. Then, the stress $\sigma(x)$ and appropriate

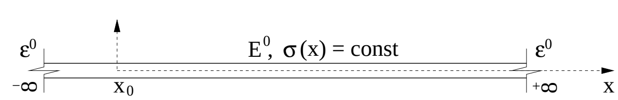

Fig. 1. Infinite homogeneous body with applied strain ε^0 at $x \to \infty$

strain $\varepsilon(x)$ inside an arbitrary point x is captured by standard *Hook's* law

$$E(x)\varepsilon(x) = \sigma(x) = \frac{q_i}{A} = \text{const}, \tag{1}$$

where $E(x) = E^0 = \text{const}$ is a smoothly redistributed material stiffness (*Young's* modulus) near the point x and q_i are the traction forces appropriate to $\sigma(x)$. Note, that in 1D the only one coordinate of the point x is measured from an arbitrarily established origin $x = 0 = x(0) = x_0$. This is sufficient information for the future BPM discretization.

J. Novák is with the Department of Mechanics, Faculty of Civil Engineering, Czech Technical University in Prague, Thákurova 7, 166 29 Prague 6, Czech Republic, e-mail: novakj@cml.fsv.cvut.cz.

Supported by research project No. 106/07/1244 and No. 1M0579
Manuscript received March 31, 2008; revised December 11, 2008.

B. Heterogeneous elastic body

In analogy with the previous section, let us introduce a similar, but heterogeneous one dimensional task as depicted in Fig. 2 Such a body differs from the homogeneous one by

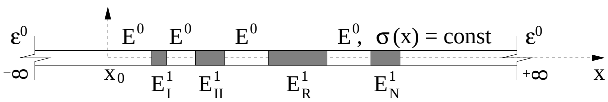

Fig. 2. Infinite heterogeneous body where the Young's modulus E^1_R is the stiffness supplement inside the domain of each perturbation $I - N$

containing a finite number of subdomains (perturbations) of finite length. The elastic stiffness is then defined by

$$E(x) = E^0 + \sum_{R=1}^{N} E^1_R(x), \tag{2}$$

where $R = 1 \ \ldots N$, and E^1_R equals zero in an entire space except the subdomains theirself. For better understanding see also the formulation for only one inclusion in Eq. (4).

C. Elastic body with one inclusion

For the sake of simplicity, the composite body shown in Fig. 2 will be reduced to a heterogeneous infinite body occupied by one inclusion as depicted in Fig. 3. The characteristic

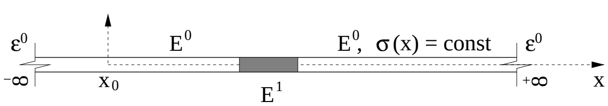

Fig. 3. Infinite heterogeneous body occupied by one inclusion with stiffness supplement E^1

function of an arbitrary point x inside the inclusion is then described by

$$V(x) : \begin{cases} V(x) = 1 & \forall x \in \Omega \\ V(x) = 0 & \forall x \notin \Omega \end{cases}, \tag{3}$$

which actually means that the function $V(x)$ equals zero in each point x outside the perturbation Ω. Having such characteristic function, Eq. (2) then easily appears as the sum of E^0 and the product of $E^1(x)$ being non-zero $\forall x$ with Eq. (3). Naturally, for the elastic body perturbed by one inclusion then holds

$$E(x) = E^0 + E^1(x). \tag{4}$$

Coupling the elastic stiffness of such laminated medium with strains and stresses considered far from the boundary of intended inclusion Γ one gets for $x \to \infty$

$$E^0(x)\varepsilon^0(x) = E^0\varepsilon^0 = \sigma(x) = \text{const.} \tag{5}$$

Eq. (5) in fact presents the same relation as valid for a homogeneous infinite medium, since, it can be assumed that the perturbation being sufficiently far from the infinite boundary does not influence the local mechanical fields at infinity.

The strain field $\varepsilon(x)$ can be decomposed in the same way as Eq. (4)

$$\varepsilon(x) = \varepsilon^0 + \varepsilon^1(x). \tag{6}$$

Then, including (4), (5) and (6) into (1) and after some simple algebraic operations as

$$\begin{aligned} E^0\varepsilon^1(x) + E^1(x)\varepsilon^0 + E^1(x)\varepsilon^1(x) &= \sigma(x) - E^0\varepsilon^0 \quad (7) \\ E^1(x)(\varepsilon^0 + \varepsilon^1(x)) &= -E^0\varepsilon^1(x) \quad (8) \\ E^0\varepsilon^1(x) &= \overline{\sigma}(x), \quad (9) \end{aligned}$$

the problem (9), to be solved, is completely formulated. Having the problem formulation and so called generalized loading such as $\overline{\sigma}(x) = -E^1(x)(\varepsilon^0 + \varepsilon^1(x))$, the solution follows the steps described in the next section.

III. Problem solution

A. Analytic solution using Fundamental Solution approach

The fundamental solution

$$\varepsilon^{1*}(x) = \frac{1}{E^0}\delta(x), \tag{10}$$

of unknown strain field $\varepsilon^1(x)$ directly follows from, see e.g. [7],

$$E^0\varepsilon^{1*}(x) = \delta(x), \tag{11}$$

where $\delta(x)$ is the unitary impulse, so called *Dirac* distribution. Solution of $\varepsilon^1(x)$ follows from application of the convolution theorem as

$$\varepsilon^1(x) = \varepsilon^{1*}(x) * \overline{\sigma}(x) = \int \frac{1}{E^0}\delta(x - x')\overline{\sigma}(x')\,\mathrm{d}x'. \tag{12}$$

Then, the right-hand side of Eq. (12) degenerates, due to the $E^1 \neq 0$ only inside the domain of inclusion, into the definite integral over Ω

$$\varepsilon^1(x) = -\int_\Omega \frac{1}{E^0}\delta(x - x')E^1(x')\varepsilon(x')\,\mathrm{d}x'. \tag{13}$$

To get the integral equation related to the local strains $\varepsilon(x)$, the $\varepsilon^0(x)$ is added to both sides of previous relation (13). Doing so, the Fredholm integral equation in terms of total strains

$$\varepsilon(x) + \frac{1}{E^0}\int_\Omega \delta(x - x')E^1(x')\varepsilon(x')\,\mathrm{d}x' = \varepsilon^0 \tag{14}$$

is formulated. Solution of the integral in equation (14) is rather simple and follows directly from the special properties of the δ-function. Considering such feature Eq. (14) can be rewritten as

$$\varepsilon(x) + \frac{1}{E^0}E^1(x)\varepsilon(x) = \varepsilon^0. \tag{15}$$

Finally, applying simple algebraic manipulations Eq. (15) becomes

$$\varepsilon(x) = \frac{E^0}{E^0 + E^1(x)}\ \varepsilon^0, \tag{16}$$

which can be declared as the exact solution of the problem (9) introduced at the end of the previous section.

B. Solution of elastic body with multiple inclusions

Of course, the solution of only one inclusion can not be sufficient for a proper description of various composite structures. On that account, an exact solution formulation of a heavily perturbed body is proceeded in this section. To derive the formulation for an elastic body occupied by N inclusions we start from (14). Particularly, it means to integrate not only over the domain of a single inclusion but over all arbitrarily redistributed subdomains $\Omega_I \dots \Omega_N$. So that rewriting Eq. (14) into

$$\begin{aligned} \varepsilon(x) &+ \frac{1}{E^0}\int_{\Omega_I} \delta(x-x')E_I^1(x')\varepsilon(x')\,\mathrm{d}x' \\ &+ \frac{1}{E^0}\int_{\Omega_{II}} \delta(x-x')E_{II}^1(x')\varepsilon(x')\,\mathrm{d}x' + \dots \\ \dots &+ \frac{1}{E^0}\int_{\Omega_N} \delta(x-x')E_N^1(x')\varepsilon(x')\,\mathrm{d}x' = \varepsilon^0, \end{aligned} \tag{17}$$

and solving all of integrals

$$\begin{aligned} \varepsilon(x) &+ \frac{1}{E^0}E_I^1(x)\varepsilon(x) + \frac{1}{E^0}E_{II}^1(x)\varepsilon(x) + \dots \\ \dots &+ \frac{1}{E^0}E_N^1(x)\varepsilon(x) = \varepsilon^0 \end{aligned} \tag{18}$$

gives the solution for the body with more inclusions

$$\varepsilon(x) = \frac{E^0}{E^0 + E_I^1(x) + E_{II}^1(x) + \dots + E_N^1(x)}\ \varepsilon^0. \tag{19}$$

Note, that the same result should be also derived in a simpler way. In particular, it is sufficient to take into account the assumption of the constant stress distribution over the whole domain of a 1D composite rod and after including Eq. (2) into Eq. (1) the formula (19) is recovered.

IV. Boundary Point Method Approximation concept

As already mentioned in Sec. **I**, the discretization approach called Boundary Point Method was developed by Russian mathematician Maz'ya. Particularly, the basis of that method was published at [1] in 1991 for the first time. The name BPM is derived from theoretically similar Boundary Element Method (BEM) and appeared after numerous discussions of Prof. Maz'ya and Dr. Khutoriansky. The principle of the method consists of the discretization of the boundary integral equations, such as is not based upon the decomposition of the boundaries into elements as known in the case of BEM, see e.q. [6]. In this approach the coefficients of the resulting algebraic system depend only on the coordinates of a finite number of boundary points and the directions of normals at these points [1, 2]. Particularly, the first step of BPM consists of the approximation of the boundary value $u(x)$ by a linear combination of basis functions $\varphi(x - x^r)$ each being concentrated near a particular boundary point and decreasing rapidly with the increasing distance $|x - x^r|$ from this point. So that, the approximation formula for a function $u(x)$ on $\mathbb{R}^d$, see e.g. [3], reaches

$$u(x) \approx u_h(x) = \sum_{r\in Z^d} u_r \varphi(x-x^r) = \sum_{r\in Z^d} u_r\varphi(x-hr), \tag{20}$$

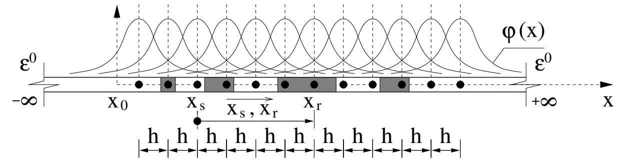

Fig. 4. Discretization scheme of unknown strains inside the infinite heterogeneous body with Gaussian basis functions (densities) at each point of discretization

and for the approximation function $\varphi(x)$ holds

$$\varphi(x) = \frac{1}{(\pi H)^{d/2}} e^{-\frac{|\mathbf{x}|^2}{Hh^2}}. \tag{21}$$

In both Eqs. (20) and Eq. (21) $r \in Z^d$ is a d-dimensional vector with integer components, hr are the coordinates of the nodes of the approximation, h is the distance between neighbor nodes of the discretization grid, $u_r = u(hr)$ is the nodal value of function $u(x)$ in the node $x = hr$ and H is the dimensionless operator regulating the Gauss "hat" opening (corresponding with *variance* parameter in case of Gauss probability function). Calculation of particular values of the discretized operators, whose densities denote the basis functions, is carried out in the second step. Of course, both steps can be performed in many different ways but in the case of a variety of material mechanics calculations the regular discretization grid is convenient to use because of the dependance of final linearized system on only equidistant distance h. Then the Fast Fourier Transform (FFT) technique can be employed to solve the final system of algebraic equations.

A. Example of known function approximation

Let us clarify a principle of previously described discretization procedure on a simple example. In particular, the function $\sin(x)$ (in sense of BPM *potential*) should be approximated as the linear combination

$$\sin(x) \approx \sin_h(x) = \sum_{r=1}^{M} \sin(hr)\varphi(x-hr), \tag{22}$$

where the shape of Gauss basis functions for 1D space reaches

$$\varphi(x-hr) = \frac{1}{\sqrt{\pi H}} e^{-\frac{|x-hr|^2}{Hh^2}}. \tag{23}$$

In spite the fact, that the Boundary Point approximation is locally convergent (for $h \to 0$, i.e. $M \to \infty$, where M is total number of nodes), for the finite number of nodes M is convergent only in average which is well seen from Fig. 5(a) where is plotted the quality of $\sin(x)$ approximation regarding the H-parameter change. On the other hand, the convergence of the approximation considering the increasing number of boundary points, while H is held constant, is expressed in Fig. 5(b). The Figures 6(a) and 6(b) show the norm, see [8]

$$\text{Norm} = \sqrt{\int_\Omega \left[\sin(x) - \sin(x)^{\text{BPM}}\right]^2 \mathrm{d}x} \tag{24}$$

of an absolute error between the discretized function and its approximation regarding the H and h variance, respectively.

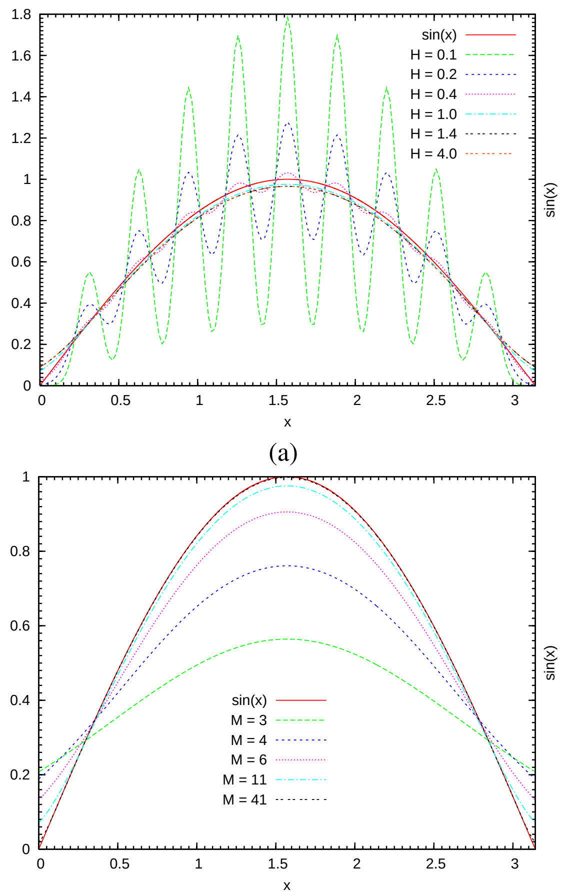

(a)

(b)

Fig. 5. BPM approximation of function $\sin(x)$, (a) approximation examples for different H–parameters, (b) approximation examples for increasing number of nodes M

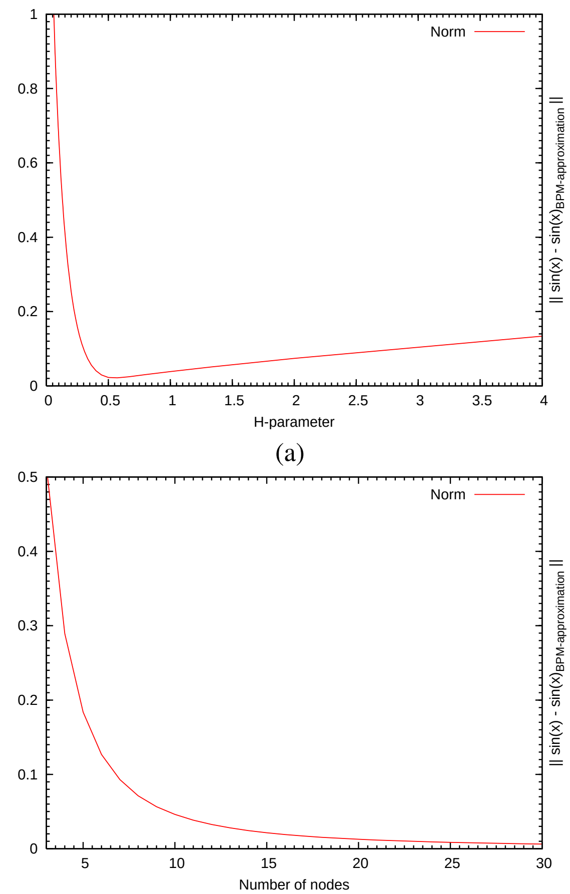

(a)

(b)

Fig. 6. Convergence of BPM approximation of function $\sin(x)$, (a) convergence of $sin(x)$ approximation to the exact function regarding the H–parameter variance, (b) convergence of $sin(x)$ approximation to the exact function regarding increasing number of discretizing nodes M

From those graphs can be seen the increasing number of nodes works really effectively while the change of H–parameter approximately over the value 1 is rather debatable.

B. Discretization of one-dimensional problem

Recall the $\sin(x)$ approximation, the unknown solution $\varepsilon(x)$ will be saught in the same way. So, according to the linearization formulas (20) and (22) the following equality can be written

$$\varepsilon(x) \approx \varepsilon_h(x) = \sum_{r=1}^{M} \varepsilon(x^r)\varphi(x - x^r) = \sum_{r=1}^{M} \varepsilon(hr)\varphi(x - hr), \tag{25}$$

thereby the unknown strain $\varepsilon(x)$ is approximated by BPM.

Owing to a particular simplicity of the analytic solution of the problem (9) respectively (14), the discretized problem can be written straightforwadly, analogically to $\sin(x)$ approximation, in the form (29). To clearly extend this theory to a more dimensional space we start from Eq. (14). After substituting for $\varepsilon(x)$ from Eq. (25) into Eq. (14) we get

$$\varepsilon_h(x^r) + \frac{1}{E^0}\int_{\Omega} \delta(x - x')E^1(x')\varepsilon_h(x'^r)\,\mathrm{d}x' = \varepsilon^0(x). \tag{26}$$

Furthermore, after integration, Eq. (26) becomes

$$\sum_{r=1}^{M} \varepsilon(x^r)\varphi(x-x^r) + \frac{1}{E^0}E^1(x^r)\sum_{r=1}^{M} \varepsilon(x^r)\varphi(x-x^r) = \varepsilon^0(x), \tag{27}$$

which can be recast as

$$\sum_{r=1}^{M} \left[1 + \frac{1}{E^0}E^1(x^r)\right]\varepsilon(x^r)\varphi(x - x^r) = \varepsilon^0(x). \tag{28}$$

As mentioned before, exactly the same expression is derived when applying the same procedure as used for the approximation of function $\sin(x)$.

$$\sum_{r=1}^{M} \frac{E^0 + E_I^1(x^r) + \cdots + E_N^1(x^r)}{E^0}\,\varphi(x^s - x^r)\varepsilon(x^r) = \varepsilon^0(x^s). \tag{29}$$

In particular, Eq. (29) is obtained including (25) to Eq. (15) or Eq. (19) and switching $x \rightarrow x^s$ in order to get the discretized problem at s independent points. Then, rewriting such equation in compact form

$$\mathsf{A}(x^s - x^r)\varepsilon(x^r) = \varepsilon^0(x^s), \tag{30}$$

the final system of linear equations is defined. Here the matrix $\mathsf{A}(x^s - x^r)$ receives the form

$$\mathsf{A}(x^s - x^r) = \sum_{r=1}^{M} \frac{E^0 + E_I^1(x^r) + \cdots + E_N^1(x^r)}{E^0}\ \varphi(x^s - x^r). \tag{31}$$

Recall Fig. 4 showing the actual sence of $\varphi(x)$ densities and x^s, x^r points as theirs variables.

V. Numerical experiments

Two important factors were tested in the framework of numerical experiments. The first one was the convergence test of, even if very simple, but practical engineering example of a laminate composite. The second, not less important step, is the advocacy of the novel *Levinson* direct solver of the *Toeplitz* structured systems of linear equations, see [10]. Those systems manifest so called *circular* properties, such as, the FFT technique may be used for a matrix–vector multiplication inside iterative solvers. In this contribution the comparative

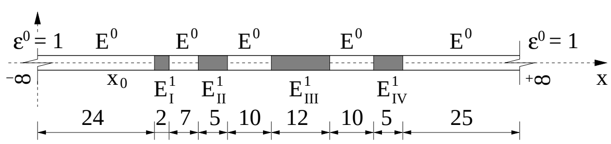

Fig. 7. Numerical experiment geometry with more inclusions of different *Young's* moduli E^i

study of the Conjugate Gradient Method (CGM) and *Levinson* direct algorithm is carried out. The most time consuming step, concretely $O(n^2)$, of CGM is the matrix–vector multiplication $\mathsf{A}\mathbf{p}_n$ where $\mathbf{p}_n$ is the direction vector and A is the matrix of the system defined by Eq. (31). Nevertheless, the multiplication has been done during all iterations using FFT technique in $O(n\log(n))$ time, see the comprehensive discussion of this topic in e.g. [9]. On the other hand, a disadvantage of iterative solvers is the worse convergence of ill–posed systems. This situation occurs for higher contrast among stiffness of the infinite reference medium and present perturbations. This contrast can be taken into account by contrast ratio

$$\mathrm{C_{ratio}} = \frac{E^0}{\widehat{E^1}} = \frac{E^0 N}{\sum\limits_{R=1}^{N} E_R^1}. \tag{32}$$

Of course, this problem is not of particular interest when using direct solvers. The beforehand mentioned *Levinson* algorithm was developed especially for the matrices exhibiting the Toeplitz properties although effective in comparison with other direct solvers sometimes shows much less efficiency then the iterative ones. On the other hand, such solver does not exhibit the convergence problems for those cases where the CGM fails.

Fig. 7 shows a simple 1D task of a prismatic area isotropic infinite rod with four inclusions given definitely by its stiffness $E^0 = 1$, $E_I^1 = 1$, $E_{II}^1 = 2$, $E_{III}^1 = 3$, $E_{IV}^1 = 4$ and geometry owing to the origin of established coordinate system. To detect the convergence behavior regarding the increasing and decreasing (both aspects have the same influence) contrast

TABLE I
10.000 nodes experiment: CGM convergence regarding the contrast ratio $\mathrm{C_{ratio}}$

E_R^1-mult.	$\mathrm{C_{ratio}}$	No. Iter.	Initial norm	Final norm
1	$1\text{x}10^{-1}$	63	$5.62\text{x}10^{2}$	$9.12\text{x}10^{-21}$
10	$1\text{x}10^{-2}$	223	$2.34\text{x}10^{3}$	$7.57\text{x}10^{-21}$
100	$1\text{x}10^{-3}$	367	$2.92\text{x}10^{3}$	$9.98\text{x}10^{-21}$
1000	$1\text{x}10^{-4}$	1000	$2.99\text{x}10^{3}$	$4.85\text{x}10^{-15}$
1500	$0.667\text{x}10^{-4}$	1000	$2.99\text{x}10^{3}$	$3.22\text{x}10^{-6}$
1600	$0.625\text{x}10^{-4}$	1000	$2.99\text{x}10^{3}$	$8.11\text{x}10^{-1}$
1700	$0.588\text{x}10^{-4}$	1000	$2.99\text{x}10^{3}$	$2.94\text{x}10^{1}$
1800	$0.556\text{x}10^{-4}$	1000	$2.99\text{x}10^{3}$	$1.28\text{x}10^{3}$
1900	$0.526\text{x}10^{-4}$	1000	$2.99\text{x}10^{3}$	$2.12\text{x}10^{13}$
2000	$0.5\text{x}10^{-4}$	1000	$2.99\text{x}10^{3}$	$2.84\text{x}10^{38}$

ratio $\mathrm{C_{ratio}}$, respectively, the Young's moduli E_R^1 has been multiplied by constant values apparent from the first column of Tab. I and Tab. II, respectively. The results of such simulations can be interpreted from Fig. 8(a), (b).

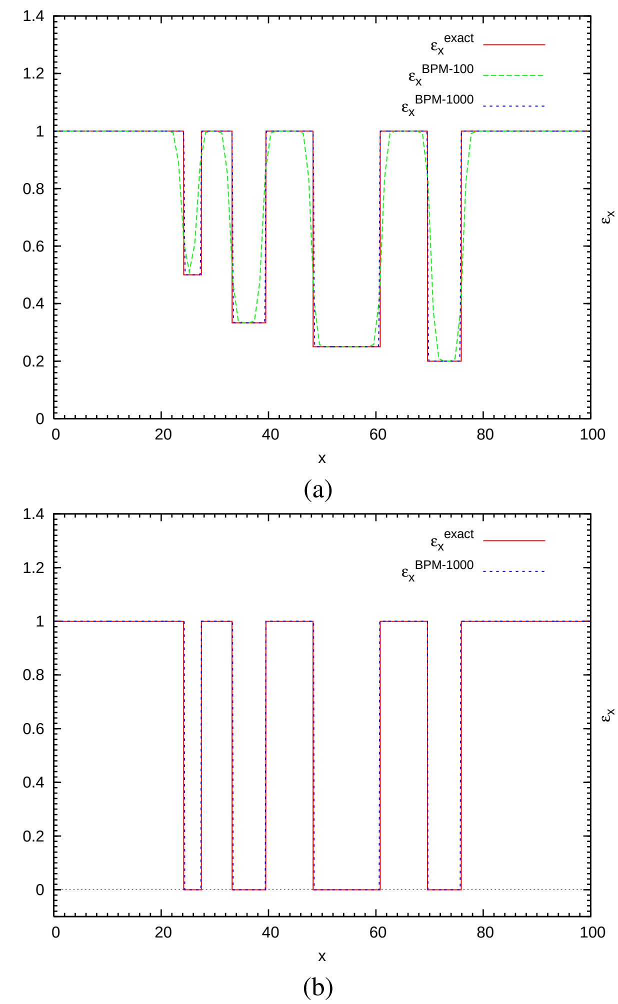

Fig. 8. Comparison of the exact and approximate solution, (a) well-posed problem (E_R^1-multiplier = 1, $\mathrm{C_{ratio}} = 1 \times 10^{-1}$) solved by CGM with respect to discretization refinement , (b) ill-posed problem (E_R^1-multiplier = 1×10^5, $\mathrm{C_{ratio}} = 1 \times 10^{-6}$) solved by *Levinson* direct solver (CGM failed)

TABLE II
100.000 NODES EXPERIMENT: CGM CONVERGENCE VERSUS LEVINSON ALGORITHM REGARDING THE CONTRAST RATIO C_{ratio}; HARDWARE CHARACTERISTICS: INTEL CENTRINO MOBILE 1.1 GHZ, 512 MB RAM

E_R^1-mult.	C_{ratio}	CGM No. Iter.	CGM time [s]	Levinson time [s]
1	1x10^{-1}	64	6.90	
10	1x10^{-2}	301	31.67	
100	1x10^{-3}	406	42.81	
200	5x10^{-3}	755	100,50	$\approx$ 120
250	4x10^{-4}	2266	297,66	
300	3.33x10^{-4}	11491	1490,28	
500	2x10^{-4}	divergence		
1000	1x10^{-4}	3810	424,26	
$\gtrapprox$1700		divergence		

VI. CONCLUSIONS AND FUTURE WORK

This article briefly presents the Boundary Point Method discretization in a simplest one-dimensional case. In spite this fact, such a short review demonstrates well aptitudes as well as apprehensive demerits of the procedure, especially regarding the lack of convergence during the use of FFT based Conjugate Gradient solver. Of course, it is possible to employ another powerful iterative solver e.g. Minimal Residual Method (MRM) such as theoretically independent on the task posedness. Although those results are not presented here, MRM has been also tried on and nowadays is still explored in the same context as here briefly presented CGM. Note, as for the solution in higher dimensioned spaces, primarily 2D and 3D, the algorithm manifests completely the same behavior as demonstrated 1D case therefore all outlined conclusions are fully portable into both 2D and 3D.

Figure 8 (a) prove quite natural property of all discretization methods that is the convergence of an approximate value $\varepsilon(x)^{\text{BPM}}$ to the exact solution $\varepsilon(x)^{\text{exact}}$ for increasing number of discretizing nodes. The convergence time of CGM has not been detected, because the solution for such small resolutions ($M = 100$ or $M = 1000$) lies over the admissible measure error of used hardware. The positive influence of nodal number increment shows Fig. 6(a, b) as well. Furthermore, the depicted results in Fig. 8 (b) advocate the use of the direct solver to process the final linearized ill-posed system. In this case the iterative CGM solver diverges, or rather totally breaks down. Contrary, in case of well-posed problems, for the contrast ratio more then 1×10^{-4} the CGM behaves stable and converges very fast after already few iteration steps, see Tab. II and Tab. I for more details. The real CGM computational times plotted at fourth column of Tab. II then shows that the BPM mesh less approximation is useful for practical applications. Namely, these data have been obtained solving the task from Fig. 7 discretized by 100.000 nodes which in fact presents the matrix of exactly same number of rows. Of course, such a matrix is not resolvable so effectively using standard linear algebra algorithms.

The outlined procedure is nowadays satisfactory done also for 2D space except for the *Levinson* or a similar direct solver. So, in regard to that, a future work will be oriented on its development. Just a note, that in a higher dimensional space the issue of using a direct solver for Toeplitz objects generated by BPM is much more complex then in 1D. With regard to that, other possibility to explore their solution via iterative preconditioned approach is availlable.

The last comment is related to positive definiteness/indefiniteness of the final matrix. This issue has not been particularly discussed in the framework of this contribution but the lack of CGM convergence seems to be due to A-matrix positive indefiniteness. The system behaves as being semidefinite. However, such a statement has to be properly explored in the future.

ACKNOWLEDGMENT

This outcome has been achieved with the financial support of the project No. 106/07/1244 and No. 1M0579. Furthermore, I would like to thank Serguei Kanaun, Sadegh Babaii and Jan Zeman for their great patience during our discussion on this topic. Considerable gratitude belongs to Jaroslav Kruis for his enthusiastic programing of the *Levinson* direct solver algorithm. Finally, the Ministry of Education, Youth and Sports, of Czech Republic and The Foreign Secretary of United States of Mexico are also gratefully acknowledged for the financial support during my stage at ITESM–CEM.

REFERENCES

[1] V. Maz'ya, *A new approximation method and its application to the calculation of volume potentials. Boundry point method*, 3. DFG–koloqium des DFG–Forschungs schwerpunktes "Randelelementmethoden", 1991.

[2] V. Maz'ya, *"Approximate approximation"*, The Mathematics of Finite Elements and Applications, Highlights, 77, 172, 1993.

[3] S. K. Kanaun, S. B. Kochekseraii, *A Numerical Method for the Solution of 3D-integral Equations of Electro-static Theory Based on Gaussian Approximating Functions*, Applied Mathematics and Computation, Elsevier, 184, 754-768, 2007.

[4] P. G. Fernando Jose, *Numerical Method for Solution of Elastic Problems of Bodies with Defects and Inclusions*, Masters thesis, ITESM-CEM, México, 2005, (in Spanish).

[5] S. K. Kanaun, V. M. Levin, *Self-Consistent Methods for Composites: Vol.1: Static Problems (Solid Mechanics and Its Applications)*, Springer, 2008 (in print).

[6] Z. S. Khodaei, J. Zeman *Microstructure-based modeling of elastic functionally graded materials: One dimensional case (2008)*, submitted for publication, preprint available at http://arxiv.org/abs/0802.0511.

[7] P. Brož, P. Procházka, *Boundary Element Method in Engineering Practice*, SNTL, 1987, (in Czech).

[8] K. Rektorys, *Variational Methods in Mathematics, Science, and Engineering*, Academia Praha, [Reidel Publishing Company], Second edition, 2001, (in Czech).

[9] Z. Tang, R. Duraiswami, N. Gumerov, *Fast algorithms to compute matrix-vector products for Pascal matrices*, Free internet resource.

[10] G. H. Golub, Ch. F. Van Loan, *Matrix Computations*, John Hopkins University Press, 3rd edition, 1996.